THE ASTROPHYSICAL JOURNAL, 419:190–196, 1993 December 10

THE [C II] 158 MICRON EMISSION FROM THE HORSEHEAD NEBULA

S. ZHOU,[1,2] D. T. JAFFE,[1] J. E. HOWE,[1,3] N. GEIS,[4,5] F. HERRMANN,[4] S. C. MADDEN,[4]
A. POGLITSCH,[4] AND G. J. STACEY[5,6]

Received 1993 March 29; accepted 1993 June 18

ABSTRACT

We have mapped the [C II] 158 μm line and observed several rotational lines of CO, ^{13}CO and CS toward selected positions in the Horsehead extinction region in IC 434. The observations show that the region has a gas density of about 10^4 cm^{-3} and an external UV flux 20–100 times the average interstellar UV field. Although this is a regime where the C^+ emission varies rapidly with UV intensity, fine-structure line emission from gas with this range of physical conditions has not been investigated previously. Comparisons of our results with models of photodissociation regions show that existing plane-parallel photodissociation region models are in general agreement with the observed intensity. It is not necessary to invoke a clumpy structure in the boundary layer to explain the observations, but the overall geometry of the cloud is important in determining the distribution of C^+ emission.

Subject headings: infrared: interstellar: lines — ISM: individual (IC 434) — ISM: molecules

1. INTRODUCTION

The [C II] $^2P_{3/2} \rightarrow {}^2P_{1/2}$ fine-structure line at 157.7 μm has been used to study a wide variety of Galactic regions and external galaxies (Howe et al. 1991; Stacey et al. 1991, and references therein). The luminosity of this line is 0.1% to 1% of the total luminosity of galaxies, and there is a good correlation between the [C II] 158 μm line intensity (I_{CII}) and the CO $J = 1 \rightarrow 0$ line intensity (I_{CO}) from a large sample of galactic regions and extragalactic nuclei (Crawford et al. 1985; Stacey et al. 1991). Wolfire et al. (1989) interpreted the correlation as a result of a common origin for these two lines: photodissociation regions (PDRs) produced by the illumination of molecular clouds by intense far-UV fluxes. Using one-dimensional models of PDRs (see Tielens & Hollenbach 1985), Wolfire et al. (1989) found that they could reproduce the observed correlation if the emitting regions have $G_0 > 10^2$ and $G_0/n > 10^{-3}$ cm^3, where G_0 is the incident far-UV radiation field in units of the equivalent average local interstellar flux (1.6×10^{-3} ergs cm^{-2} s^{-1}; see Habing 1968) and n is density in units of H atoms per cm^3 (the density of molecular gas defined as particles per cm^3 is $\sim 0.6n$).

The one-dimensional PDR models successfully explain the intensity of the [C II] emission observed in regions with strong far-UV radiation (e.g., Galactic OB star–forming regions and extragalactic starburst nuclei; Stacey et al. 1991), although they have difficulties explaining the depth of the emitting region into the cloud (Stutzki et al. 1988; Howe et al. 1991; Stacey et al. 1993). The models also can account for the measured [C II] intensities of molecular interfaces near B stars in reflection nebulae with values of G_0 from a few 10^2 to 10^3 (Chokshi et al. 1988; Jaffe et al. 1990) where both the [C II]/CO $1 \rightarrow 0$ ratio and the logarithmic dependence of I[C II] on G_0 are similar to what one sees in the high G_0 regime. Models covering low to moderate densities (10^2–10^4 cm^{-3}) and radiation fields below $G_0 = 10^2$ (Sternberg & Dalgarno 1989; Hollenbach, Takahashi, & Tielens 1991) show that the [C II] line intensity varies roughly linearly with G_0 for values between ~ 10 and 100, while the intensity of the CO $1 \rightarrow 0$ transition varies much more slowly. Up to now, there have been few detailed studies of [C II] line sources with low UV fluxes, because the lines are weak and it is difficult to observe the often highly extended sources in the far-IR.

In this paper, we present [C II] observations toward the Horsehead Nebula. The optical nebula IC 434, located at a distance of 475 pc, extends over 1° on the plane of the sky. We concentrate on a $\sim 10'$ section of the nebula centered on the horsehead-shaped extinction region. Within the extinction region, there is dense gas ($\sim 10^4$ cm^{-3}); to the west, the gas column density drops sharply. These are characteristics of a true cloud edge. There are several young stars forming in the mapped portion the cloud, all of low luminosity (Reipurth & Bouchet, 1984; Sandel et al. 1986). From the projected distances to ζ and σ Ori, we estimate G_0 at the cloud surface to be about 20–100 (see § 3.1). The simplicity of the region makes it an ideal laboratory for testing models of PDRs in regions with small ambient UV fields. In addition, studies of this low-UV intensity regime are relevant both to a wide range of galactic molecular cloud interfaces and to the interpretation of emission from galaxies, many of which have global values of G_0 within the range found in the Horsehead Nebula (Madden et al. 1993; Stacey et al. 1990). In particular, Stacey et al. (1991) propose the use of the [C II]/CO ($J = 1 \rightarrow 0$) line intensity ratio as a diagnostic of global star-formation activity in galaxies. Determination of this ratio in Galactic regions with low UV intensity and no star formation is an important reference point for the diagnostic.

Maps of [C II] emission can also probe the structure near cloud edges. Previous far-IR fine-structure line studies have produced useful information about the excitation and energetics of cloud surfaces (Stutzki et al. 1988; Howe et al. 1991; Meixner et al. 1992; Stacey et al. 1993), but the observations were toward regions with very high incident UV fields (10 to 10^3 times that of the Horsehead Nebula) and high densities,

[1] Department of Astronomy, University of Texas, Austin, TX 78712-1083.
[2] Department of Astronomy, University of Illinois, Urbana, IL 61801.
[3] Department of Astronomy, University of Maryland, College Park, MD 20742.
[4] Max-Planck-Institut für Extraterrestrische Physik, D-8046 Garching bei München, Germany.
[5] Department of Physics, University of California, Berkeley, Berkeley, CA 94720.
[6] Department of Astronomy, Cornell University, Ithaca, NY 14853-6801.

such as M17 SW and the Orion Bar. Cloud edges away from luminous star-forming regions have been studied in CO lines by Falgarone, Phillips, & Walker (1991), who find the structure to be both complex and hierarchical. [C II] observations provide another way to study the structure of cloud surfaces. The Horsehead region has a density comparable to the regions studied by Falgarone et al. (1991).

2. OBSERVATIONS AND RESULTS

We made the [C II] 158 μm observations using the Max-Planck-Institut für Extraterrestrische Physik/University of California at Berkeley Far-Infrared Fabry-Perot spectrometer (FIFI) (Poglitsch et al. 1991) on the NASA Kuiper Airborne Observatory (KAO) in 1991 September. FIFI has a 5 × 5 focal plane array with detectors spaced by 40″. The beam size for each detector is 55″ (FWHM) and the beam shape is approximately Gaussian (68″ equivalent disk; $\Omega = 8.3 \times 10^{-8}$ sr). The Lorentzian instrumental profile gave a 51 km s^{-1} spectral resolution. To preserve our sensitivity to extended low-level emission, we observed sources by switching the bandpass of the Fabry-Perot filter between a reference frequency and an observing frequency at ~10 Hz while sweeping the observing frequency of the Fabry-Perot filter across the [C II] line. The maximum spectral switch was ±3.2 resolution elements. We subtracted residual baseline curvature by taking frequency-switched scans on blank sky ~1° west of the Horsehead. Typical integration times were 10 minutes per array placement. The data were calibrated by observing an internal blackbody source about once every hour. We derived the correction for telescope and instrument throughput from observations of Mars to obtain a relation between the blackbody signal and an absolute intensity scale. The calibration uncertainty is ~30%, and the absolute pointing uncertainty is ≤15″.

Figure 1 shows a contour map of the [C II] 158 μm integrated line intensity superposed on the Palomar Observatory Sky Survey (POSS) O-print. The peak [C II] intensity is 4.3×10^{-4} ergs cm^{-2} s^{-1} sr^{-1} with a noise level about 10% of the peak intensity. Systematic uncertainties in the baseline rather than random noise from the thermal background dominate the overall noise level.

Using the 10.4 m telescope of Caltech Submillimeter Observatory (CSO)[7] and the 30 m telescope of Institut de Radio Astronomi Millimetrique (IRAM), we also observed the Horsehead Nebula in lines of CO and CS. Table 1 summarizes the parameters for the molecular and [C II] line observations.

The ^{12}CO and ^{13}CO $J = 2 \rightarrow 1$ observations were made at 30″ intervals along a right ascension cut with $\delta = -02°28'30''$ in 1991 November at the CSO. These observations had a spatial resolution of 30″ and a spectral resolution of 1.3 km s^{-1}. Table 2 lists the results of the CO cut. To get the radiation temperature T_{mb}, we divided T_A^* (obtained at the telescope) by 0.71, the main beam efficiency at 230 GHz (J. G. Mangum, private communication).

We observed eight points in the CS $J = 2 \rightarrow 1$, $3 \rightarrow 2$, and $5 \rightarrow 4$ lines in 1991 October at IRAM. Figure 2 shows the positions observed in CS superposed on the contour map of [C II] emission. Table 1 lists the beam sizes, velocity resolutions, and main beam efficiencies; Table 3 gives the results of the CS observations. Note that the velocity of the CS $J = 2 \rightarrow 1$ line appears to be redshifted by 0.2 km s^{-1} with respect to the $J = 3 \rightarrow 2$ line. This shift was seen in all sources observed on the same run and is probably caused by an error in the observing frequencies. Zhou et al. (1993), whose CS observations were obtained on the same observing run, give more details about the observations.

[7] The CSO is operated by the California Institute of Technology under funding from the National Science Foundation, contract AST 90-15755.

TABLE 1

OBSERVATIONAL PARAMETERS

Line Name	Telescope	Resolution ΔV (km s^{-1})	Beam	Efficiency η_{mb}
[C II] $^2P_{3/2} \rightarrow {}^2P_{1/2}$	KAO	51	55″	...
CO (2 → 1)	CSO	0.13	30	0.71
^{13}CO (2 → 1)	CSO	0.13	30	0.71
CS (2 → 1)	IRAM	0.12	24	0.68
CS (3 → 2)	IRAM	0.20	17	0.68
CS (5 → 4)	IRAM	0.12	11	0.49

3. DISCUSSION

3.1. *The Nature of the Horsehead*

The Horsehead region in Figure 1 is on the western edge of the Orion B molecular cloud (L1360). The optical nebula west of this cloud, IC 434, appears to be ionized gas streaming into a low-density region. The edge of the molecular cloud runs north-south in the plane of the sky, marked by a sharp cutoff in optical emission on the POSS plates. The Horsehead is an optical extinction and molecular emission region which extends into IC 434 across an otherwise straight boundary.

The Orion B molecular cloud, including the Horsehead region, has been mapped in the CO and ^{13}CO $J = 1 \rightarrow 0$ lines (Stark & Bally 1982; Maddalena et al. 1986) and the CS $J = 2 \rightarrow 1$ line (Lada, Bally, & Stark 1991) with beam sizes of 1′.8 or larger. These studies place the Horsehead near the edge of the CO emitting region, coincident with a CS clump (clump 42 of Lada et al. 1991) which has a size of 0.2 pc and a virial mass of 35 $M_\odot$.

TABLE 2

CO OBSERVATIONS

R.A.[a] (5^h38^m)	^{12}CO DATA V (km s^{-1})	ΔV (km s^{-1})	T_A^* (K)	$I = T_A^* \Delta V$ (K km s^{-1}) ^{12}CO	^{13}CO	I (C II) (10^{-4} ergs cm^{-2} s^{-1} sr^{-1})
17^s.4.....	5.3	2.7	1.9	9.4	1.0	1.1
19.4.....	5.3	3.0	1.7	11.4	2.1	1.4
20.4.....	10.9	2.6	3.0	18.5	2.0	1.6
21.4.....	10.8	2.3	7.7	19.0	9.0	1.7
22.4.....	10.8	2.4	14.9	45.4	9.8	2.0
23.4.....	11.0	2.5	17.5	54.1	11.7	2.0
25.4.....	11.0	2.5	12.4	50.4	4.2	2.0
27.4.....	10.8	2.4	11.1	35.3	8.7	1.9
29.4.....	10.5	2.6	9.7	30.0	8.3	2.2
31.4.....	10.6	2.7	10.1	31.4	11.1	3.0
33.4.....	10.6	2.9	11.1	37.9	10.4	3.2
35.4.....	10.6	2.8	11.2	36.0	8.4	3.2
37.4.....	10.7	2.7	10.8	40.3	9.2	1.8
39.4.....	10.6	2.6	10.5	35.6	8.3	1.4
41.4.....	10.6	2.9	9.6	29.7	8.8	...
43.4.....	10.7	2.9	10.5	36.4	8.2	...
45.4.....	10.9	3.2	11.1	44.3	9.1	...
47.4.....	11.6	3.9	14.8	71.6	12.6	...

[a] All points have $\delta = -2°28'30''$ and the same hour and minute in right ascension.

1993ApJ...419..190Z

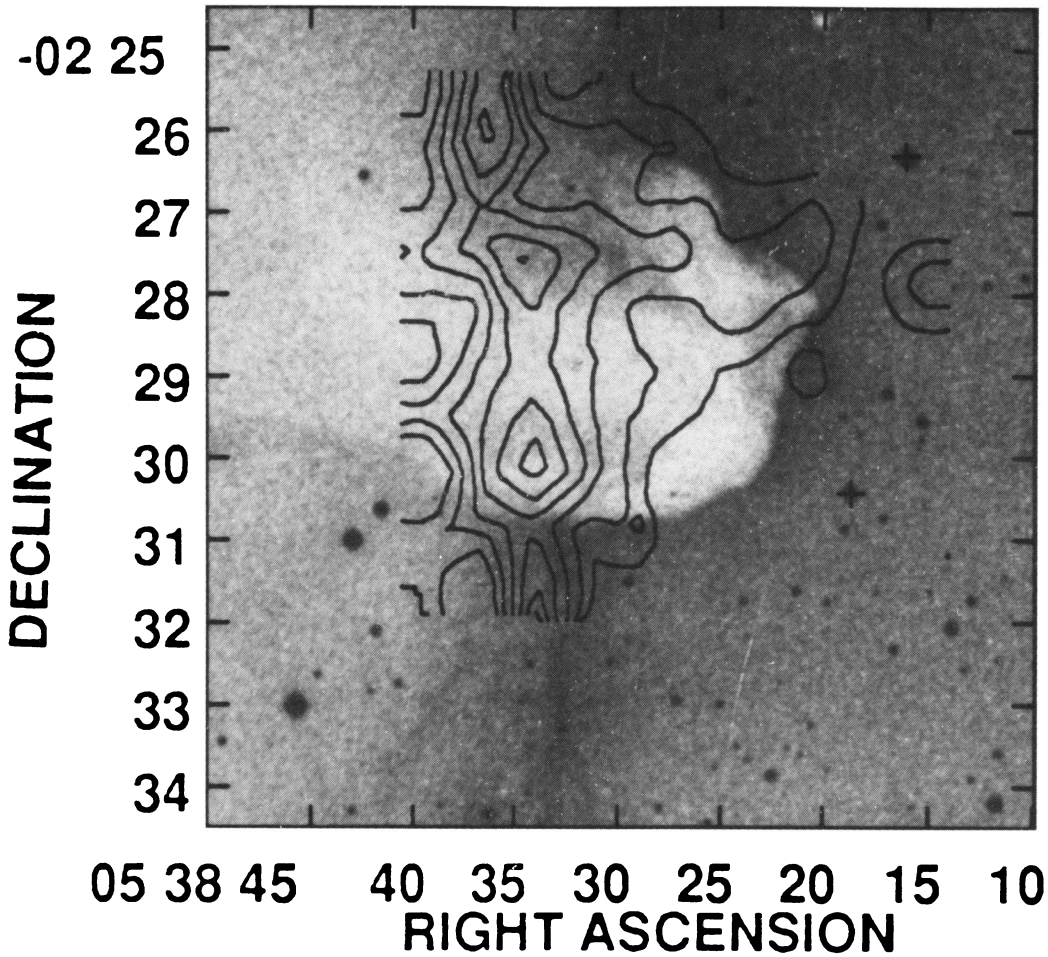

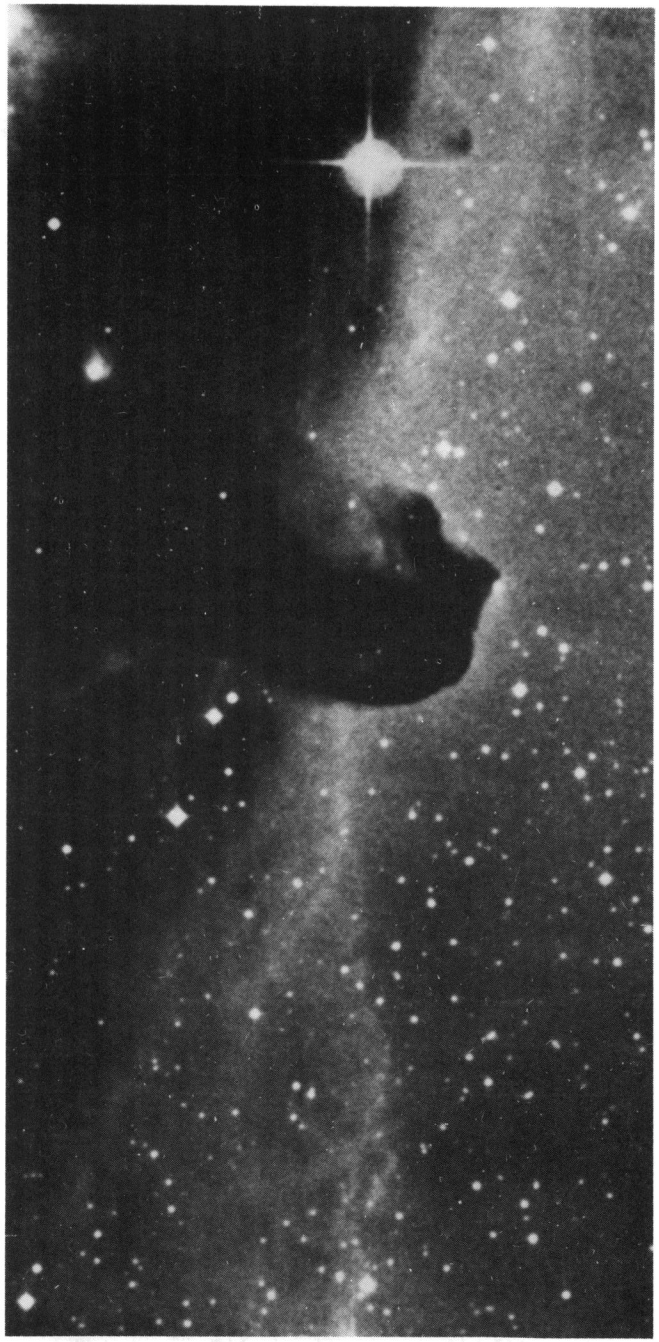

FIG. 1.—(*left*) Map of the [C II] 158 μm integrated intensity overlaid on the POSS O-plate of the Horsehead Nebula. The contour interval is 5×10^{-5} starting at 1.5×10^{-4} ergs cm^{-2} s^{-1} sr^{-1}. (*right*) Larger scale image of the same region showing the relationship of the Horsehead to the extended north-south optical ionization front (photo courtesy of the Royal Observatory, Edinburgh, and the Anglo-Australian Telescope Board).

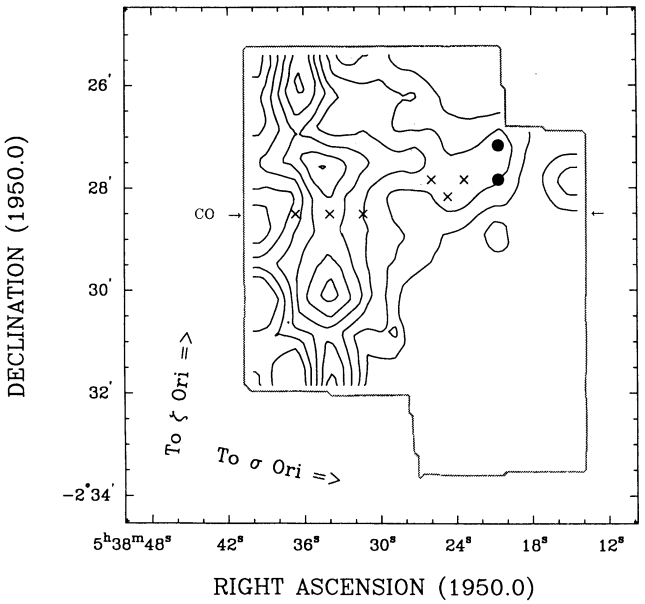

FIG. 2.—[C II] integrated intensity map as in Fig. 1. The crosses mark the positions where the CS lines were detected, and the dots mark the positions for which there are CS upper limits. The small arrows mark the position of the CO cut. The large arrows indicate the directions to ζ Ori and σ Ori.

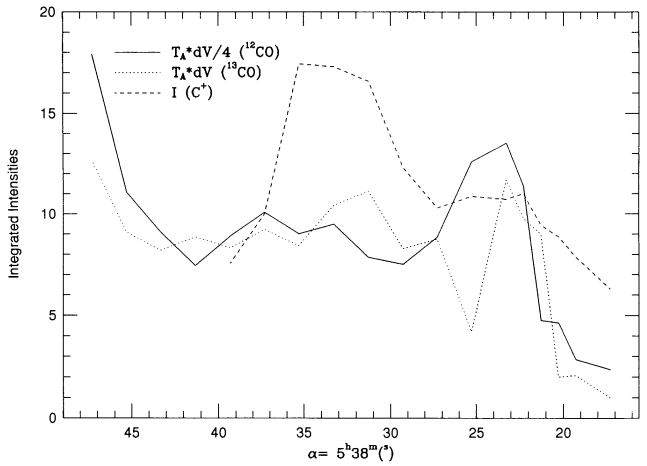

FIG. 3.—Integrated intensities of the [C II] 158 μm line, CO, and ^{13}CO $J = 2 \rightarrow 1$ lines along a cut at constant declination $\delta = -02°28'30''$. The CO and ^{13}CO intensities are in units of K km s^{-1}, and the [C II] intensities are in units of 2.5×10^{-5} ergs cm^{-2} s^{-1} sr^{-1}.

Our higher resolution CO data (Table 2) show strong CO emission at 10.5 km s^{-1} extending from the main body of the cloud out to the western edge of the Horsehead, where the CO intensity drops sharply (Fig. 3). The CO intensity does not drop to zero west of the Horsehead, however. There is weak CO emission at 5.5 km s^{-1}, which partially overlaps the 10.5 km s^{-1} emission. Our CS data (Table 3) show emission at ~10 km s^{-1}, which disappears beyond the western edge of the Horsehead. The weak CO emission at 5.5 km s^{-1} likely arises elsewhere along the line of sight, separated from the CS emission region.

From the CS line temperatures in Table 3, we estimate the volume density of molecular gas and the CS column density using a large velocity gradient model similar to those described in Snell et al. (1984). The derived volume densities cluster around 2×10^4 cm^{-3} (Table 3); the total mass derived by multiplying the density by the volume gives ~40 $M_\odot$, similar to the virial mass (Lada et al. 1991). The agreement of the two mass estimates implies a gas volume filling factor of nearly 1. The high volume filling factor means that, unlike in the clouds modeled by Stutzki et al. (1988) and Howe et al. (1991), there is not much opportunity for UV photons striking the envelope of the Horsehead to penetrate for long distances without intercepting the dense gas.

The primary sources of UV radiation are the binary system ζ Ori (O9.5 Ibe and B0 III) to the north and σ Ori (O9.5 V) to the west (spectral types from Warren & Hesser 1977; directions toward the stars are marked in Fig. 2); both are about 0°.5 (4 pc, projected on the sky) away from the Horsehead. The UV radiation from the embedded infrared sources is insignificant. Assuming the stars and the nebula are in the same plane perpendicular to the line of sight with no extinction between them, the incident far-UV flux would range from $G_0 = 60$ to 90—higher toward the northwest. We derived these far-UV fluxes by summing the contributions from ζ and σ Ori assuming that the stars radiate like blackbodies at the effective temperatures appropriate for their spectral type (Panagia 1973; Morton & Adams 1968) and purely geometric dilution of the radiation field. If dust absorption in the cloud is considered, the UV intensity would be much lower than 60 toward the south and east.

3.2. *The* [C II] *Emission and Comparison with Models*

The [C II] emission in Figure 1 can be divided into two parts: an east-west protrusion along the northern edge of the

TABLE 3

CS OBSERVATIONS[a]

		CS $J = 2 \rightarrow 1$			$J = 3 \rightarrow 2$			$J = 5 \rightarrow 4$		
α (5^h38^m)	δ ($-2°$)	V (km s^{-1})	ΔV (km s^{-1})	T_A^* (K)	V (km s^{-1})	ΔV (km s^{-1})	T_A^* (K)	T_A^* (K)	log n (cm^{-3})	log N (cm^{-2})
20.7.....	27.8	...	...	<1.2	...	...	<0.8	<1.8	...	...
20.7.....	27.2	...	...	<1.2	...	...	<0.8	<1.8	...	...
23.4.....	27.8	10.8	0.66	3.1	10.5	0.82	1.5	≤1.8	4.5	13.9
24.7.....	28.2	10.6	0.73	4.2	10.5	0.74	2.6	<1.8	3.9	14.7
26.0.....	27.8	10.5	0.72	3.2	10.3	0.64	2.3	<1.8	4.7	13.8
31.4.....	28.5	10.4	0.63	2.8	10.1	0.77	1.9	<1.8	4.5	13.9
34.0.....	28.5	10.3	0.77	2.7	10.2	0.90	1.6	<1.8	3.9	14.5
36.7.....	28.5	10.5	0.76	2.2	10.3	0.93	0.9	<1.8	4.9	13.5

[a] Observed points are marked in Fig. 2.

Horsehead and a narrow north-south ridge. We compare our observations with PDR models, which give the emergent [C II] 158 μm line intensity (when viewed face-on) from a plane-parallel medium with a constant n (density) and G_0. While the model geometry is much simpler than in real clouds, the models show how the [C II] line intensity should vary with the local UV intensity and gas density.

3.2.1. *The E-W Protrusion*

According to the PDR models (Hollenbach et al. 1990; Sternberg & Dalgarno 1989; see also Fig. 5 of Wolfire, Hollenbach, & Tielens 1990), the [C II] line intensity is roughly linear in G_0 but independent of n for $10 < G_0 < 100$ and $n \sim 10^4$ cm^{-3}. Since the gas density in the Horsehead Nebula is about 10^4 cm^{-3} (Table 3), the [C II] intensity distribution should follow the UV intensity distribution, i.e., the strongest [C II] emission should come from the northwestern edge of the Horsehead, where the cloud surface is perpendicular to the direction to ζ Ori. Indeed, the E-W protrusion of [C II] emission is coincident with the northern edge of the Horsehead. The intensity is about 2.5×10^{-4} ergs cm^{-2} s^{-1} sr^{-1}, similar to the model prediction (see Fig. 5 of Wolfire et al. 1990) of 3×10^{-4} for $G_0 = 100$ and $n = 10^4$ cm^{-3}. The models of Sternberg & Dalgarno (1989) predict a somewhat lower [C II] intensity due to the high degree (0.1) of carbon depletion they assume. At the western and southern edges of the Horsehead protrusion, the extinction between ζ Ori and the cloud surface is nonnegligible and the small local UV intensity ($G_0 \lesssim 20$) comes primarily from σ Ori. The predicted [C II] intensity is $\leq 1.0 \times 10^{-4}$ ergs cm^{-2} s^{-1} sr^{-1}, consistent with our nondetection.

3.2.2. *The Ridge of C^+ Emission*

The strongest emission in our map comes from the [C II] ridge along $\alpha = 05^h38^m35^s$. The peak intensity is 4.3×10^{-4} ergs cm^{-2} s^{-1} sr^{-1}. The true intensity could be somewhat higher because the ridge is only marginally resolved east-west. At the middle of the mapped portion of the ridge, $G_0 \sim 70$, with the majority of the far-UV coming from ζ Ori and the balance from σ Ori. Plane-parallel PDR models predict a face-on [C II] intensity of $\sim 2.5 \times 10^{-4}$ over $10^3 \leq n(H_2) \leq 10^5$ cm^{-3} (Wolfire et al. 1990), only slightly less than the observed peak intensity. The direction to ζ Ori, however, forms an angle of only 10° with the ridge, so that the effective UV intensity is only ~ 40. How does the orientation of the ridge with respect to ζ Ori and the elongated geometry of the emission region affect the relationship between the observed and predicted intensities? Particularly, why is the observed emission from the Horsehead similar to the predicted value while the observed ridge emission is brighter?

The narrow [C II] emission ridge is a separate entity from the E-W protrusion. The ridge is part of a longer structure, seen in a larger scale [C II] map of the NGC 2024 region (Jaffe et al. 1993), which continues to the north and marks the boundary between the optical nebula and the molecular cloud. The partially ionized region parallels the $\sim 1°$ long filaments of ionized gas apparent in optical photographs (see inset in Fig. 1). The Horsehead, which lies in front of the filaments, has high enough optical extinction to interrupt the continuity of the visible filaments but transmits the [C II] emission from the ridge. The lack of the CS $J = 2 \rightarrow 1$ line emission from a molecular counterpart to the [C II] filament (Lada et al. 1991) indicates that the density in the ridge is significantly less than that of the Horsehead. With this picture in mind, we investigate various effects of geometry on the [C II] intensity.

Let us look at the true [C II] intensity distribution prior to the convolution with the telescope beam. Consider a simple picture of the ridge as a plane-parallel interface of finite depth, edge-on to the line of sight. In this picture, the exciting star is at the same distance from us as the interface but distant from the cloud edge as compared to the depth of the interface. If we begin with the star at a position where it shines directly down on the interface and move it in the plane of the sky toward the actual 10° angle of ζ Ori, the UV flux at the cloud surface drops as cos θ, where θ is the angle from the normal to the interface. The result of this lower UV flux is a drop in the face-on [C II] intensity of the cloud (the intensity as viewed from a position in the plane of the sky) by a corresponding factor. Looking at the interface edge-on, we also see the amount of UV radiation striking the cloud per unit area decrease by cos θ if scattering of UV photons is insignificant. Note, however, that the oblique incidence angle results in a shorter penetration scale length for the UV by cos θ. Although less total energy per unit area is deposited in the cloud, this reduced scale length means that the *absorbed energy* per unit distance into the cloud has the same value at the cloud surface as in the normal incidence case but drops more quickly into the cloud. Viewed from the edge, the peak of the true [C II] surface brightness (without beam smearing) is therefore independent of θ. It is the thickness of the emitting layer that drops as cos θ.

After convolving with the telescope beam, a resolved ridge will appear narrower as θ increases, but the peak brightness and the shape of the brightness distribution will not change. An unresolved ridge will drop in [C II] flux in proportion to cos θ. We do not have a good estimate of the density of the molecular gas in the ridge behind the Horsehead. The lack of the CS $J = 2 \rightarrow 1$ emission only requires that this gas be significantly less dense than the Horsehead. For a density of 3×10^3 cm^{-3} and normal incidence of the exciting UV radiation, a PDR should emit significant amounts of [C II] to a depth of ~ 0.44 pc (Hollenbach et al. 1990). At $\theta = 10°$, this scale would drop to 0.08 pc, or 35″ at 475 pc. Observed with our beam, the maximum observed [C II] intensity would be diluted down by 35/60, or 0.6, as a result of this effect.

There is another way to look at this geometric effect. Assuming a planar interface viewed edge-on with an effective normal incident flux already corrected for cos θ, we can bring the models into agreement with the [C II] observations by recognizing the need to correct the intensities upward by a factor of sec ϕ (ϕ is angle between the normal to the cloud surface and the line of sight) before comparing with observations. When ϕ is close to 90°, which is likely the case for the narrow emission ridge, the observed intensity is limited by the optical depth of the [C II] line. To explain the observed emission in this way, a factor of 2 enhancement is needed in the [C II] intensity, implying that the optical depth of the [C II] line must be less than 0.7 when viewed face-on. Stacey et al. (1991) have estimated an optical depth ~ 1 for the Orion A interface near θ_1 C Ori. The value for the Horsehead ridge, if viewed face-on, should be lower.

The above discussion treats the cloud boundary as a flat surface, almost parallel to the line of sight, which may be an oversimplification. Even if the [C II] emission arises from the surface of a filament instead of a slab, PDRs can have a significant amount of limb brightening over a large range of orientations. A filament with UV incident from one side which has a

PDR with a depth equal to 25% of its radius will have a [C II] emission path length up to six times longer than that of a face-on plane-parallel PDR. In short, the bright [C II] ridge can be explained by emission arising from a cloud boundary viewed edge-on.

3.3. C^+ *Emission as a Probe of Cloud Structure*

In PDRs the C^+ ions exist only on the surfaces of dense cloud or cloud cores. For a clumpy cloud edge illuminated by intense UV radiation, the lower density interclump medium could be ionized, leaving thin layers of C^+ on the surface of individual dense clumps. By mapping the [C II] emission at high spatial resolution, we should, in principle see outlines of individual clumps. A good example is shown by our map of the Horsehead region, where the E-W protrusion marks the northern boundary of the optical extinction region (which is also a CS clump in Lada et al. 1991) toward the star ζ Ori—the source of the UV radiation.

Even when [C II] observations are unable to resolve individual clumps, the penetration depth of UV photons into the cloud, as revealed by the extent of the [C II] emission, should shed light on the clumpiness of the cloud. In the PDRs of NGC 1977 and W3, Howe et al. (1991) found that [C II] emission extends over 1–10 parsecs into the dense molecular cloud, about one order of magnituder farther than the UV penetration depth into a uniform medium. Using a clumpy cloud model, they were able to reproduce strength and distribution of the observed [C II] emission.

In the cloud interface region behind the Horsehead, we found that the [C II] emission is confined to a narrow ridge, consistent with a cloud edge of uniform density at 3×10^3 cm^{-3} (see § 3.2). Do the observations, then, rule out the existence of clumpy structure shown by Falgarone et al. (1991)? Not necessarily. Following the formulation of Howe et al. (1991), in a cloud edge consisting of opaque clumps and negligible interclump medium, we find an UV attenuation length ($1/e$; no geometric dilution) of D/f_v, where D is the diameter of the opaque clumps and f_v is the volume filling factor. In the case of the narrow ridge, we require that D/f_v be 0.1 pc or less. Therefore, if the smallest clump in the cloud is 0.1 pc, the filling factor must be close to 1, i.e., the cloud is not clumpy. However, if the clump size is as small as 0.02 pc (Falgarone et al. 1991), the volume filling factor could be as small as 0.2. In short, the extent of [C II] emission may be used to infer clumpiness; but, when clumpiness is not required, the data cannot be used to rule out clumpiness on scales significantly smaller than the beam size.

3.4. *The Correlation of* [C II] *with* CO

Figure 3 shows the integrated intensities of ^{12}CO $J = 2 \rightarrow 1$, ^{13}CO $J = 2 \rightarrow 1$, and [C II] lines along a line of constant declination $\delta = -02°28'30''$. The [C II] emission has a peak around $\alpha = 05^h38^m35^s$, which corresponds to the ridge in Figure 1, and decreases slowly toward the western edge of the Horsehead. The ^{12}CO and ^{13}CO intensities are fairly uniform across the ridge of [C II] emission, rise slightly near the western edge of the Horsehead, and drop sharply at the edge. The CO intensities also rise toward the main body of the Orion B molecular cloud to the east ($\Delta\alpha > -500''$), where no [C II] data are available.

The intensity ratio I_{CII}/I_{CO} varies from 300 (equivalent intensity units) in the ridge of [C II] emission to 1500 near the edge of the Horsehead. Note that one can understand the higher ratio in the ridge as a consequence of less saturation (caused by high optical depth) in the [C II] emission than in the CO emission in an edge-on geometry. Since the ^{12}CO $J = 2 \rightarrow 1$ is quite optically thick (^{12}CO to ^{13}CO ratio is about 4; see Fig. 3), the intensities of ^{12}CO $J = 2 \rightarrow 1$ and $1 \rightarrow 0$ are approximately the same. Hence, we can compare our [C II] to CO ratio to those derived from CO $J = 1 \rightarrow 0$ line intensities. Crawford et al. (1985) first noted a tight correlation between the integrated intensities of the [C II] 158 μm line and the CO $J = 1 \rightarrow 0$ line, with an average ratio of 4400 (after converting CO antenna temperature to main-beam brightness temperature), for Galactic OB star-forming regions and starburst galaxies. Stacey et al. (1991) found a ratio of ~1300, with considerable scatter for cool dust galaxies. The ratio in the Horsehead region is similar to the ratio in the nuclei of cool dust galaxies, indicating that the average molecular interstellar medium in cool dust galactic nuclei may be clouds with moderate density exposed to UV fields of $G_0 \sim 10$–100. The variations of the line intensity ratio in our data (factor of 2) are also present in the observations of the nuclei of cool dust galaxies.

Wolfire et al. (1989) interpreted the tight correlation found in starburst galaxies and Galactic OB star–forming regions in terms of a common beam filling factor for both the [C II] and CO emission when both G_0 and n are high and a common critical density when G_0 is high and n is low. The necessary physical condition for the correlation to hold is $G_0 > 10^2$ and $G_0/n > 10^{-3}$ cm^3. The Horsehead region, having $G_0 = 20$–80 and $n \sim 10^4$ cm^{-3}, marks the critical regime where the correlation begins to break down. The lower I_{CII}/I_{CO} ratio in the Horsehead is consistent with the interpretation of Wolfire et al. (1989). Alternatively, Burton, Hollenbach, & Tielens (1990) found that molecular self-shielding becomes important at $G_0/n > 10^{-2}$ cm^3; hence, molecular self-shielding may also be responsible for the low I_{CII}/I_{CO} ratio in the Horsehead.

4. SUMMARY

We have mapped the Horsehead Nebula in the [C II] 158 μm line. The emission shows up along the northern edge of the Horsehead as well as in a north-south ridge across the neck of the Horsehead. Several rotational lines of CO, ^{13}CO, and CS have also been observed toward selected positions. We inferred a gas volume density of $\sim 10^4$ cm^{-3} from the CS observations. Inside the Horsehead, the distribution of molecular material is fairly uniform with a sharp cutoff beyond the optical extinction region. Combined with the calculated UV intensity, we find the observed [C II] emission consistent with current PDR models and that carbon is not significantly depleted in the C^+ region. At the cloud interface behind the Horsehead, the distribution of [C II] emission is consistent with a cloud edge of uniform density but does not rule out clumpiness on small scales (0.01 pc). The intensity ratio I_{CII}/I_{CO} varies from 1500 to 3000; the larger value is primarily caused by geometric enhancements in the observed [C II] emission. These values are similar to the values for cool dust galaxies but lower than those for galactic OB star–forming regions and starburst galaxies (Stacey et al. 1991).

This work was supported by NASA grant NAG 2-402 and NSF grant AST 9017710 to the University of Texas at Austin. S. Z. acknowledges support from NASA POS-46462-E, the Laboratory for Astronomical Imaging at the University of Illinois, and NSF AST 90-24603.

REFERENCES

Burton, M. G., Hollenbach, D. J., & Tielens, A. G. G. M. 1990, ApJ, 365, 620
Chokshi, A., Tielens, A. G. G. M., Werner, M. W., & Castelaz, M. W. 1988, ApJ, 313, 853
Crawford, M. K., Genzel, R., Townes, C. H., & Watson, D. M. 1985, ApJ, 291, 755
Falgarone, E., Phillips, T., & Walker, C. 1991, ApJ. 378, 186
Habing, H. J. 1968, Bull. Astron. Inst. Netherlands, 19, 421
Hollenbach, D. J., Takahashi, T., & Tielens, A. G. G. M. 1991, ApJ, 377, 192
Howe, J. E., Jaffe, D. T., Genzel, R., & Stacey, G. J. 1991, ApJ, 373, 158
Jaffe, D. T., et al. 1993, ApJ, in preparation
Lada, E. A., Bally, J., & Stark, A. 1991, ApJ, 368, 432
Maddalena, R. J., Morris, M., Moscowitz, J., & Thaddeus, P. 1986, ApJ, 303, 375
Madden, S. C., Geis, N., Genzel, R., Herrmann, F., Jackson, J., Poglitsch, A., Stacey, G. J., & Townes, C. H. 1993, ApJ, 407, 579
Meixner, M., Haas, M. R., Tielens, A. G. G. M., Erickson, E. F., & Werner, M. 1992, ApJ, 390, 499
Morton, D. C., & Adams, T. F. 1968, ApJ, 151, 611
Panagia, N. 1973, AJ, 78, 929
Poglitsch, A., et al. 1991, Int. J. Infrared Millimeter Waves, 12, 859
Reipurth, B., & Bouchet, P. 1984, A&A, 137, L1
Sandell, G., Reipurth, B., Walmsley, C. M., & Ungerechts, H. 1986, in Light on Dark Matter, ed. F. P. Israel (Dordrecht: Reidel), 295
Snell, R. L., Mundy, L. G., Goldsmith, P. F., Evans, N. J., & Erickson, N. R. 1984, ApJ, 276, 625
Stacey, G. J., Geis, N., Genzel, R., Jackson, J. M., Poglitsch, A., & Townes, C. H. 1990, in Proc. 29th Liège Int. Ap. Colloq., ed. B. Kaldeich (Paris: European Space Agency), 85
Stacey, G. J., Geis, N., Genzel, R., Lugten, J. B., Poglitsch, A., Sternberg, A., & Townes, C. H. 1991, ApJ, 373, 423
Stacey, G. J., Jaffe, D. T., Geis, N., Genzel, R., Poglitsch, A., & Townes, C. H. 1993, ApJ, 404, 219
Stark, A. A., & Bally, J. 1982, in Regions of Recent Star Formation, ed. R. S. Roger & P. E. Dewdney (Dordrecht: Reidel), 329
Sternberg, A., & Dalgarno, A. 1989, ApJ, 338, 197
Stutzki, I., Stacey, G. J., Genzel, R., Harris, A. I., Jaffe, D. T., & Lugten, J. B. 1988, ApJ, 332, 379
Tielens, A. G. G. M., & Hollenbach, D. J. 1985, ApJ, 291, 722
Warren, W. H., Jr., & Hesser, J. E. 1977, ApJS, 34, 115
Wolfire, M. G., Hollenbach, D., & Tielens, A. G. G. M. 1989, ApJ, 344, 770
Wolfire, M. G., Tielens, A. G. G. M., & Hollenbach, D. 1990, ApJ, 358, 116
Zhou, S., Evans, N. J., II, Kömpe, C., & Walmsley, C. M. 1993, ApJ, 404, 232

Note added in proof.—We underestimated the UV flux at the Horsehead Nebula by a factor of 2 in § 3.1. An incorrect luminosity class for the supergiant ζ Ori was used in the calculations, but the error is compensated in part by a line-of-sight distance of ≥ 4.4 pc between ζ Ori and the Horsehead Nebula (see Jaffe et al. 1993). The main conclusions are not affected by this error.